1 **New particle formation events observed at King Sejong Station,**

2 **Antarctic Peninsula – Part 1: Physical characteristics and contribution**

3 **to cloud condensation nuclei**

4

5 Jaeseok Kim[1,2], Young Jun Yoon[1,*], Yeontae Gim[1], Jin Hee Choi[1], Hyo Jin Kang[1,3], Ki-Tae Park[1],

6 Jiyeon Park[1], and Bang Yong Lee[1]

7

8 [1]Korea Polar Research Institute, 26 Songdomirae-ro, Yeonsu-gu, Incheon 21990, Republic of Korea

9 [2]Korea Research Institute of Standards and Science, 267 Gajeong-ro, Yuseong-gu, Daejeon 34113,

10 Republic of Korea

11 [3]University of Science & Technology (UST), 217 Gajeong-ro, Yuseong-gu, Daejeon 34113, Republic

12 of Korea

13 *Correspondence to*: Young Jun Yoon (yjyoon@kopri.re.kr)

14

15 **Abstract**

16   The physical characteristics of aerosol particles during a particle burst observed at King Sejong

17 Station in Antarctic Peninsula from March 2009 to December 2016 were analyzed. This study focuses

18 on the seasonal variation in parameters related to particle formation such as the occurrence, formation

19 rate (FR) and growth rate (GR), condensation sink (CS), and source rate of condensable vapor. The

20 number concentrations during new particle formation (NPF) events varied from 1707 cm^{-3} to 83120

21 cm^{-3}, with an average of 20649 ± 9290 cm^{-3}, and the duration of the NPF events ranged from 0.6 h to

22 14.4 h, with a mean of 4.6 ± 1.5 h. The NPF event dominantly occurred during austral summer period

23 (~72%). The mean values of FR and GR of the aerosol particles were 2.79 ± 1.05 cm^{-3} s^{-1} and 0.68 ±

24 0.27 nm h^{-1}, respectively showing enhanced rates in the summer season. The mean value of FR at King

25 Sejong Station was higher than that at other sites in Antarctica, at 0.002-0.3 cm^{-3} s^{-1}, while those of

26 growth rates was relatively similar results observed by precious studies, at 0.4~4.3 nm h^{-1}. The average

27 values of CS and source rate of condensable vapor were (6.04 ± 2.74) × 10^{-3} s^{-1} and (5.19 ± 3.51) ×

28 10^4 cm^{-3} s^{-1}, respectively. The contribution of particle formation to cloud condensation nuclei (CCN)

29 concentration was also investigated. The CCN concentration during the NPF period increased

1   approximately 9% compared with the background concentration. In addition, the effects of the origin

2   and pathway of air masses on the characteristics of aerosol particles during a NPF event were

3   determined. The FRs were similar regardless of the origin and pathway, whereas the GRs of particles

4   originating from the Antarctic Peninsula and the Bellingshausen Sea, at 0.77 ± 0.25 nm h^{-1} and $0.76 \pm$

5   0.30 nm h^{-1}, respectively, were higher than those of particles originating from the Weddell Sea ($0.41 \pm$

6   0.15 nm h^{-1}).

7

8   **1. Introduction**

9   Understanding the effect of atmospheric aerosol particles on climate change is an important issue

10   in atmospheric science. These particles are highly significant substances in the radiation transfer

11   process in the atmosphere, with direct effects through scattering and absorption of solar radiation and

12   indirect effects by acting as cloud condensation nuclei (CCN) for cloud droplets (Anttila et al., 2012).

13   These particles also influence the properties and life time of clouds (Twomey, 1977; Albrecht, 1989).

14   Although aerosol particles play an important role in global and regional climates, large uncertainties

15   remain owing to a lack of knowledge on their formation and physicochemical characteristics (Carslaw

16   et al., 2013; IPCC, 2013).

17   New particle formation (NPF) frequently occurs in the atmosphere and leads to enhancement of the

18   total number concentrations of aerosol particles due to high numbers of nucleation mode particles

19   (Spracklen et al., 2006; Dall'osto et al., 2017). The modeling study of Pierce and Adams (2007)

20   indicates that new ultrafine particles of <100 nm can contribute to maximum CCN generations of 40%

21   and 90% at the boundary layer and in the remote free troposphere, respectively. In order to understand

22   the characteristics of the NPF, studies have been conducted in various regions including coastal, forest,

23   mountainous, rural and urban sites (O'Dowd et al., 2002; Komppula et al., 2003; Kulmala et al., 2004;

24   Yoon et al., 2006; Park et al., 2009; Kim et al., 2011; Rose et al., 2015; Bianchi et al., 2016; Kontkanen

25   et al., 2017). In addition, studies on the NPF phenomenon have recently been conducted at various

1   sites in the polar regions (Asmi et al., 2010; Järvinen et al., 2013; Kyrö et al., 2013; Park et al., 2004;

2   Weller et al., 2015; Humphries et al., 2016; Nguyen et al., 2016; Willis et al., 2016; Barbaro et al.,

3   2017; Dallósto et al., 2017). A NPF event occurring form December 1998 to December 2000 at the

4   South Pole was reported by Park et al. (2004). Kyrö et al. (2013) showed that oxidized organics derived

5   from the oxidation of biogenic precursors originating from local melting ponds might have contributed

6   to particle growth at the Finnish research station Aboa (73.50°S, 13.42°W). In addition, studies on the

7   NPF were conducted at the Concordia station, Dome C (75.10°S, 123.38°E; Järvinen et al., 2013) and

8   at the coastal Antarctic station Neumayer (70.65°S, 8.25°W; Weller et al., 2015). Although studies on

9   NPF events have been conducted at various stations in the Antarctica, no results are available for the

10   station in the Antarctic Peninsula. Also, the contribution of NPF to CCN concentration is not well

11   understood in this area. Furthermore, results of the general long-term characteristics of aerosol

12   particles during the period of NPF observation in Antarctica are rare compared with those in other

13   continents.

14   In the present study, the frequency of NPF events was determined on the basis of total aerosol

15   number concentration. We investigated the physical characteristics such as formation rate (FR) and

16   growth rate (GR), condensation sink (CS) and source of condensation vapor as well as the seasonality

17   of atmospheric aerosols during NPF events at King Sejong Station in the Antarctic Peninsula. The

18   effect of particle formation on CCN concentrations was also examined. Furthermore, the air mass back

19   trajectories were analyzed by using the Hybrid Single Particle Lagrangian Integrated Trajectory

20   (HYSPLIT) model to understand physical properties of NPF events depending on the origins and

21   pathway of the air masses.

22

23   **2. Methods**

24   **2.1. Site description and instrumentation**

25   The data analyzed in this study were obtained at the King Sejong station in the Antarctic Peninsula

1   (62.22°S, 58.78°W). Further details on the sampling site as well as the instrumental set-up were

2   introduced in our previous study (Kim et al., 2017). In brief, two condensation particle counters (CPCs;

3   TSI 3776 and TSI 3772) were used to measure the total particle number concentrations. The size

4   distributions of the aerosol particles ranging from 10 nm to 300 nm were measured by using a scanning

5   mobility particle sizer (SMPS), which combined a differential mobility analyzer (DMA; HCT Inc.,

6   LDMA 4210) and a CPC (TSI 3772). The CCN concentrations were determined by using a CCN

7   counter (CCNC; DMT CCN-100). In addition, meteorological parameters including temperature,

8   relative humidity, wind speed, wind direction, pressure, and solar radiation intensity were continuously

9   monitored by using an automatic weather station (AWS; Vaisala HMP45 for measuring temperature

10   and relative humidity, WeatherTronics 2102 for measuring wind speed and direction, WeatherTronics

11   7100 for measuring pressure and Eppley Precision Spectral Pyranometer PSP for measuring solar

12   radiation intensity) system.

13
14   **2.2. Data analysis**

15   To ensure data quality, raw data of the following conditions were discarded: (i) wind direction

16   between 355° and 55° (local pollution sector) (ii) concentration of black carbon higher than 100 ng m⁻

17   ^{3}, (iii) wind speed less than 2 m s^{-1} and (iv) instrument malfunction based on the log-book. If valid data

18   for one day were less than 50% after discarding the raw data, such days were excluded. The acquisition

19   rate for each instrument is summarized in Table 1. Here, the acquisition rate indicates the value of the

20   analyzed days divided by the total measurement days. Because the acquisition rate from the SMPS

21   was lower than that of the CPC in this study, the value difference between the concentrations of

22   particles larger than 2.5 nm ($CN_{2.5}$) and 10 nm (CN_{10}) observed from two CPCs was used to identify

23   the NPF events.

24
25   **2.2.1. Definition of NPF events**

26   As mentioned in the previous section, the value difference between $CN_{2.5}$ and CN_{10} concentrations

Atmospheric
Chemistry
and Physics
Discussions

1   were used to define days for NPF events or non-NPF events (Yoon et al., 2006). The value difference

2   (CN$_{2.5}$-CN$_{10}$) represents the number concentrations of newly formed particles produced from gas-to-

3   particle conversion. The NPF days were defined in this study according to the following conditions:

4   (i) The difference in number concentrations (CN$_{2.5}$-CN$_{10}$) is higher than 500 cm^{-3} (ii) the (CN$_{2.5}$-

5   CN$_{10}$)/CN$_{10}$ ratio is higher than 10 and (iii) the NPF duration is longer than 30 min. The (CN$_{2.5}$-

6   CN$_{10}$)/CN$_{10}$ ratio is the parameter used to distinguish between particles newly formed from gas-to-

7   particle conversion and background particles (Warren and Seinfeld, 1985; Humphries et al., 2015).

8   Humphries et al. (2016) also used the (CN$_{2.5}$-CN$_{10}$)/CN$_{10}$ ratio to distinguish the NPF days during a 52

9   days voyage in the East Antarctic sea ice region because the number concentration data were more

10   reliable than the size distribution data.

11

12   **2.2.2. Classification of NPF events using SMPS data**

13   After identification of the NPF event days, classification of the NPF events was conducted by using

14   size distributions from a SMPS. The NPF events were classified into three types of A, B and C

15   according to the classification by Dal Maso et al. (2005) and Yli-Juuti et al. (2009). Type A describes

16   days in which the formation and growth of particles were clear. Type B describes days in which the

17   formation occurred but growth was not clear. Type C describes days in which the event occurrence

18   was not distinct.

19

20   **2.2.3. Estimation of parameters for NPF characteristics**

21   On the basis of the number concentration data with 1 s time resolution the FR was calculated for

22   cases in which the concentrations of (CN$_{2.5}$-CN$_{10}$) sharply increased. The FR of new particles ranging

23   from 2.5 nm to 10 nm was determined according to variation in the number concentrations of CN$_{2.5-10}$

24   (CN$_{2.5-10}$=CN$_{2.5}$-CN$_{10}$) based on the following equation (Dal Maso et al., 2005):

25

26    $$FR = \frac{dN_{nuc}}{dt} + F_{coag} + F_{growth} \qquad (1)$$

Atmospheric
Chemistry
and Physics
Discussions

1

2   Here, N_{nuc} is the particle number concentrations of nucleation mode. In this study, the $CN_{2.5-10}$

3   concentrations obtained by two particle counters were used for the term N_{nuc}. F_{coag} is the particle loss

4   in accordance with coagulation, and F_{growth} represents the flux of particles growing from the nucleation

5   mode. Because the $CN_{2.5-10}$ concentrations were predominant in the total number concentration and

6   the particles rarely grew over the nucleation mode during the formation period, the F_{coag} and F_{growth}

7   terms in Eq. 1 were neglected in this study (Dal Maso et al., 2005; Shen et al., 2016).

8   The GRs were calculated by using the size distributions measured by a SMPS. In order to calculate

9   the geometric mean diameter (GMD) as a function of time, we chose the particle range of 10-20 nm

10   due to the size resolution of the SMPS. The GR was determined by rate of change in the GMD by

11   using the following equation (Kulmala et al., 2004; Dal Maso et al., 2005):

12

13
$$GR = \frac{dD_p}{dt} \tag{2}$$

14

15   The CS is an important parameter governing the NPF because it indicates the speed in which

16   gaseous molecules condense onto pre-existing aerosols. It can be estimated from the size distribution

17   data according to the following equation (Dal Maso et al., 2005; Kulmala et al., 2005; Shen et al.,

18   2016):

19

20
$$CS = 2\pi D \sum_{dp} \beta_m d_p N_{dp} \tag{3}$$

21

22   where D is the diffusion coefficient of the condensable vapor, β is the transitional regime correction

23   factor from Fuchs and Sutugin (1970), and d_p and N_{dp} are the particle size and number concentration,

24   respectively. It is assumed that condensable vapor is gaseous sulfuric acid which has been reported to

25   play an important role in the nucleation process (Dal Maso et al., 2005).

Atmospheric
Chemistry
and Physics
Discussions

1   According to the GR and the CS, it is possible to estimate condensable vapor concentration, C_v (unit:

2   molecules cm^{-3}) and its source rate, Q (unit: molecules cm^{-3} s^{-1}; Kulmala et al., 2001; Dal Maso, 2002),

3   assuming that the particle growth is caused by condensation of a low volatile vapor to the particle

4   surface. In the nucleation mode, the relationship between C_v and GR is estimated by the following

5   equation:

6

7    $$C_v = A \times GR \qquad\qquad (4)$$

8

9   where A is a constant, specifically 1.37×10^7 h cm^{-3} for a vapor with the molecular properties of sulfuric

10   acid. It assumed that C_v is constant during the growth process.

11   Assuming no other sink terms for the condensing vapor, source rate of condensable vapor is

12   estimated under the steady-state condition:

13

14    $$Q = CS \times C_v \qquad\qquad (5)$$

15

16   **2.3. Backward trajectory analysis**

17   To understand characteristics of NPF events depending on the origin and pathway of air masses, air

18   mass backward trajectory analysis was performed by using the HYSPLIT model (Stein et al., 2015;

19   http://www.arl.noaa.gov/HYSPLIR.php). Typical 48-h air mass backward trajectories were analyzed,

20   ending at heights of 100m, 500m, and 1500m above the ground level of the sampling site. The results

21   with similar air mass origins and pathways during the NPF periods at three different heights were used

22   for the analysis in this study. Accordingly, the air mass was categorized into four cases according to its

23   origin and pathway: two affected continents including South America and the Antarctic Peninsula and

24   two affected marine cases including the Weddell and Bellingshausen Sea (Fig. 1).

25

26   **3. Results and discussion**

27   **3.1 Characteristics of the NPF events**

3.1.1 Occurrence frequency and FR of NPF events

After data screening as mentioned in the previous section, 1655-days of data recorded during the observation periods from March 2009 to December 2016 were analyzed. The data including valid data were classified into two groups, NPF event days and non-event days, by using $CN_{2.5-10}$ concentrations measured by two CPCs. The duration of the NPF ranged from 0.6 to 14.4 h, with a mean of 4.6 ± 1.5 h. Only 6.1% (101 days) of the results were defined as NPF events, whereas 93.9% (1554 days) were classified as the non-NPF events (Table 2). This NPF frequency at King Sejong Station in the Antarctic Peninsula is quite low compared with those in previous studies at other mid-latitude sites (Kulmala et al., 2004; Dal Maso et al., 2005; Pierce et al., 2014; Rose et al., 2015); comparison with other sites in the Antarctic is difficult owing to the lack of long-term observed results. In addition, the monthly variation of the NPF frequency was compared as shown in Fig. 2. It is clear that the NPF number was highest during the austral summer, from December to February, whereas non-events were observed in the austral winter period from June to August. Approximately 72% of the NPF occurred during the summer period, showing the highest value of 38% in January. The clear difference in the frequency of the NPF events in austral summer and winter periods should speculates that solar intensity and temperature play important roles in the formation and growth of aerosol particles, along with precursor vapors derived from marine biota activities in the Antarctic (Virkkula et al., 2009; Kyrö et al., 2013; Weller et al., 2015; Jang et al., 2018).

The FR of particles ranging from 2.5 nm to 10 nm varied from 0.16 to 9.88 cm^{-3} s^{-1}, with an average of 2.79 ± 1.05 cm^{-3} s^{-1}. Fig.3 shows the monthly variations in the FR over whole observation periods. The seasonal trend in the FR shows a pattern similar to that of the NPF events frequency. The FRs were the highest during the austral summer (December-February, 3.20 ± 1.09 cm^{-3} s^{-1}). Those in the austral autumn period (March-May, 1.71 ± 0.56 cm^{-3} s^{-1}) were similar to those of the spring period (September-November, 1.71 ± 0.79 cm^{-3} s^{-1}). Because the NPF was observed only one case in May, the result of the May data was ignored in this analysis. In particular, the monthly maximum FR in

1   December and the minimum in October were 3.52 cm^{-3} s^{-1} and 0.84 cm^{-3} s^{-1}, respectively. The FR

2   measured at various stations in the Antarctic and other continents are summarized in Table 3. The

3   average level of the FR observed in this study was more than 10 times higher than that of other stations

4   in Antarctica. Although it is difficult to directly explain the causes of the higher FR, it is likely that the

5   method used in this study to derive the FR influenced the results. The FRs were estimated in the

6   previous studies on the basis of the size distribution data with few minute time resolution, whereas the

7   FR in this study was calculated by using the variation in total number concentration (CN$_{2.5-10}$) data

8   with a time resolution of 1 s. Another possible reason is the location. As shown in Table 3, the FR at a

9   coastal region, specifically Mace Head located approximately 500 m from the coast, is higher than that

10   reported at other sites due to the high biological activity of marine algae, which produce gaseous

11   precursors from tidal zone and open oceans. Previous modeling research showed that the dimethyl

12   sulfide emission in the Antarctic Peninsula during the astral summer period is higher than that in other

13   regions in Antarctica (Yu and Luo, 2010). Thus, the characteristics of the sampling site might have

14   caused the FR to be higher than that at other site in Antarctica.

15

16   **3.1.2 Calculation of other parameters based on size distribution data**

17   On the basis of the size distribution results measured with a SMPS, NPF events were categorized

18   into three NPF types, as mentioned as Sect. 2.2.2. Type C (which is undefined days) was dominant, as

19   shown in Table 4; among all NPF event days, only two days (2.0%) were considered as Type A events.

20   The GRs of nucleation mode particles ranged between 0.02 nm h^{-1} and 3.09 nm h^{-1}, with a mean of

21   0.68 ± 0.27 nm h^{-1}. Fig. 4(a) presents the monthly variation in the GR from March 2009 to December

22   2016. A seasonal trend in the GR is apparent, in which the maximum occurred in the summer. The GR

23   gradually began to decrease in February whereas and increase again in November, as shown in Fig.

24   4(a). The GR in January was 0.76 ± 0.26 nm h^{-1}, whereas that in November was 0.40 ± 0.15 nm h^{-1}.

25   The GR in this study is similar to the values reported in previous studies conducted in Antarctica. For

Atmospheric
Chemistry
and Physics
Discussions

1   instance, Weller et al. (2015) reported that the GR at the Neumayer station varied between 0.4 and 1.9

2   nm h^{-1}, with an average of 0.90±0.46 nm h^{-1}. However, our results are lower than those reported by

3   Järvinen et al. (2013), who studied NPF events at Concordia station, Dome C from December 2007 to

4   November 2009 and showed a GR of 4.3 nm h^{-1}. This discrepancy is likely attributed to the number of

5   analyzed days. In the present study, we analyzed 86 of 101 NPF days, whereas the previous study

6   analyzed 15 NPF days.

7   Fig. 4(b) shows a monthly variation in CS during NPF events. The CS varied from 0.02×10^{-3} s^{-1}

8   to 25.66×10^{-3} s^{-1}, with an average of $(6.04 \pm 2.74) \times 10^{-3}$ s^{-1}. The value was high in February ((8.17 ±

9    $3.55) \times 10^{-3}$ s^{-1}) and a low in April (($2.44 \pm 0.70) \times 10^{-3}$ s^{-1}), as shown in Fig. 4(b). The CS measured

10   in this study was approximately 5-10 times higher than that observed at the other Antarctic station.

11   Weller et al. (2015), who estimated the CS using light scattering data measured from Neumayer station,

12   indicated a CS value of about 10^{-3} s^{-1}. A median CS value of 4.0×10^{-4} s^{-1} in a 47-day observation period

13   at Aboa station was reported by Kyrö et al. (2013). Järvinen et al. (2013) also showed a CS value of

14   1.8×10^{-4} s^{-1} using data of 15 days.

15   The monthly variation in the condensable vapor source rate during an NPF event is displayed in

16   Fig. 4(c). The source rates derived were between 0.03×10^3 and 3.74×10^5 cm^{-3} s^{-1}, with a mean source

17   rate of $(5.19 \pm 3.51) \times 10^4$ cm^{-3} s^{-1}. The source rate of condensable vapor was maximum during the

18   austral summer months. In particular, the maximum and minimum average values of the source rate

19   were $(6.40 \pm 3.43) \times 10^4$ cm^{-3} s^{-1} in January and $(1.93 \pm 0.92) \times 10^4$ cm^{-3} s^{-1} in November, respectively.

20   This source rate was higher than that measured at a coastal Antarctic station. Kulmala et al. (2005)

21   reported that the value of source rate varied from 0.9×10^3 cm^{-3} s^{-1} to 2.0×10^4 cm^{-3} s^{-1} at the Aboa station.

22

23   **3.3 CCN concentration during NPF events**

24   In this section, the contribution of particle formation to the variation in CCN concentration is

25   investigated. Although recent studies reported that number concentrations of climate-relevant particles

1   increased during NPF events (Pierce et al., 2014; Shen et al., 2016; Rose et al., 2017), the contribution

2   of NPF to CCN concentration was estimated by using an indirect method. The number concentrations

3   of particles larger than 50, 80 and 100 nm were estimated by using size distribution data. That value

4   was considered as potential CCN concentration at different supersaturation value. In this study,

5   however, CCN concentrations at a supersaturation value of 0.4% were measured. Fig. 5 shows

6   variation in normalized values of $CN_{2.5-10}$ and CCN concentrations as a function of time. The

7   normalized value was calculated from $CN_{2.5}$ and the CCN concentration at each time divided by the

8   concentration recorded 1 h prior to the NPF event. The zero in the x-axis in the figure represents the

9   start time of the NPF event. Data for only 34 days out of 101 NPF days were valid due to the CCN

10 data availability limited by a malfunctioning of an instrument. The $CN_{2.5-10}$ concentrations sharply

11 increased at NPF start time and the peak concentration occurred 2 h afterward, as shown in Fig. 5.

12 Moreover, the CCN concentrations gradually increased for 9 h. Indeed, the maximum CCN

13 concentrations rose from $170.7 \pm 38.6 cm^{-3}$ to $185.6 \pm 44.6 \ cm^{-3}$ during and after the NPF events,

14 respectively, showing an increase of 9%.

15

16 **3.4 Effects of air mass origin on NPF events**

17   The effects of air mass origin on the NPF characteristics were also investigated by 48-h air mass

18 back trajectory analysis. The frequencies of NPF, FR, GR, CS, and the source rate of condensable

19 vapor over the whole observation period are listed in Table 5. Here, the analysis results of the NPF

20 characteristics of air masses originating from South America (Case I) and in an undefined case are not

21 shown owing to low frequencies. The air masses originating from the sea (Case II and IV) were

22 dominant during NPF event at King Sejong Station. The FRs were analogous regardless of the air mass

23 origin and pathway, while the GR of Case III and Case IV was significantly higher than those of Case

24 II. The lower GR should be related to the CS and the source rate of condensable vapor. In the case of

25 the air mass originating from the Weddell Sea (Case II), the CS was higher than that of other cases,

1   whereas the source rate of condensing vapor was lowest. The higher CS and lower source rate might

2   a indicate decline in condensing vapor and hence a decrease in GR. Our results for the source rate of

3   condensable vapor agree with those of a previous study by Yu and Luo (2010), discussed the role of

4   dimethyl sulfide (DMS) emission in the NPF process in remote oceans. In their simulation study, the

5   concentrations of DMS and sulfuric acid in the Bellingshausen Sea and the Antarctic Peninsula area

6   during the austral summer season were higher than those in Weddell Sea region. In satellite-derived

7   estimates of the biological characteristics, DMS produced from phytoplankton was found to be more

8   dominant in the Bellingshausen Sea than in the Weddell Sea (Jang et al., 2018). Sulfuric acid is derived

9   from oxidation of DMS in oceans (Virkkula et al., 2009). In this study, the condensable vapor was

10   assumed to be sulfuric acid in the source rate calculations, as mentioned in Sect. 2.2.3.

11   Fig. 6 shows a comparison of the NPF characteristics depending on the origin and pathway of the

12   air mass during the summer season. The mean CS value was high. However, in case of the air mass

13   originating from the Bellingshausen Sea (Case IV), the GR was relatively higher than the values of air

14   masses originated from other region due to the higher values of the source rate of condensable vapor.

15   The mean value of this source rate for the air mass originating from the Weddell Sea (Case II) was

16   similar to that from the Antarctic Peninsula (Case III), while the CS mean value was 1.7 times higher.

17   This resulted in a low GR.

18   For air mass originating from the Bellingshausen Sea (Case IV), the seasonal properties of the

19   parameters related to the NPF events were analyzed. As shown in Fig. 7, the mean values of FR, GR

20   and the source rate of condensable vapor were highest during the austral summer periods. However,

21   mean values of CS were highest during the spring period.

22

23   **4. Summary**

24   In this study, the characteristics of NPF at King Sejong station in Antarctic Peninsula were

25   investigated using a data set of eight years from March 2009 to December 2016, of total particle

Atmospheric
Chemistry
and Physics
Discussions

Open Access

EGU

1   number concentrations and particle size distributions. The frequencies of NPF events and FR were

2   obtained by using the data of total number concentrations, whereas GR, CS and the source rate of

3   condensable vapor were calculated from the aerosol size distribution results. A low occurrence

4   frequency of NPF events, at 6%, was observed, and most of the NPF events occurred during the austral

5   summer. No NPF events were observed during the winter due to lower solar radiation and a lack of

6   precursors for particle formation. The mean values of the FR and GR were 2.79 ± 1.05 cm^{-3} s^{-1} and

7   0.68 ± 0.27 nm h^{-1}, respectively. These results show that the FR at King Sejong Station as higher than

8   that at other Antarctica sites, whereas the GR was relatively similar to values reported in previous

9   studies conducted in the Antarctic. A possible reason for the lower GR can be attributed to the CS,

10   which was 5-10 times higher than that reported at other stations in Antarctica. This observation

11   suggests that condensable vapor contributed to growth of nucleated nanoparticles and may have

12   condensed onto pre-existing particles, hence decreasing the GR. According to 48-h backward

13   trajectory analysis, air masses originating from oceanic areas were dominant during the NPF events.

14   In order to investigate the contribution of the NPF events to variation in CCN concentrations at a

15   supersaturation value of 0.4%, the CCN concentrations were compared with the CN$_{2.5-10}$

16   concentrations as a function of time. The results showed that the CCN concentrations during and after

17   the NPF events increased approximately 9% compared with those measured before the event. This

18   study is the first to report the characteristics of NPF in the Antarctic Peninsula. However, further

19   research is need to understand the chemical characteristics of aerosol particles and the chemical

20   composition of precursors during NPF events to fully understand the NPF for this region.

21

22   **Author contributions**

23   JK and YJY designed the study, YG, JHC, HJK, KTP, JP, and BYL analysed aerosol data. JK and

24   YJY prepared the manuscript with contributions from all co-authors.

25

26   **Acknowledgements**

Atmospheric
Chemistry
and Physics
Discussions

4

5   **References**

6   Albrecht, B. A.: Aerosols, cloud microphysics, and fractional cloudiness, Science, 245, 1227-1230,
7   10.1126/science.245.4923.1227, 1989.
8   Anttila, T., Brus, D., Jaatinen, A., Hyvärinen, A.-P., Kivekäs, N., Romakkaniemi, S., Komppula, M.,
9   and Lihavainen, H.: Relationships between particles, cloud condensation nuclei and cloud droplet
10   activation during the third Pallas Cloud Experiment, Atmos. Chem. Phys., 12, 11435–11450,
11   https://doi.org/10.5194/acp-12-11435-2012, 2012.
12   Asmi, E., Frey, A., Virkkula, A., Ehn, M., Manninen, H. E., Timonen, H., Tolonen-Kivimäki, O.,
13   Aurela, M., Hillamo, R., and Kulmala, M.: Hygroscopicity and chemical composition of antarctic
14   sub-micrometre aerosol particles and observations of new particle formation, Atmos. Chem. Phys.,
15   10, 4253-4271, 10.5194/acp-10-4253-2010, 2010.
16   Barbaro, E., Padoan, S., Kirchgeorg, T., Zangrando, R., Toscano, G., Barbante, C., and Gambaro, A.:
17   Particle size distribution of inorganic and organic ions in coastal and inland Antarctic aerosol,
18   Environ. Sci. Pollut. Res., 24, 2724-2733, 10.1007/s11356-016-8042-x, 2017.
19   Bianchi, F., Tröstl, J., Junninen, H., Frege, C., Henne, S., Hoyle, C. R., Molteni, U., Herrmann, E.,
20   Adamov, A., Bukowiecki, N., Chen, X., Duplissy, J., Gysel, M., Hutterli, M., Kangasluoma, J.,
21   Kontkanen, J., Kürten, A., Manninen, H. E., Münch, S., Peräkylä, O., Petäjä, T., Rondo, L.,
22   Williamson, C., Weingartner, E., Curtius, J., Worsnop, D. R., Kulmala, M., Dommen, J., and
23   Baltensperger, U.: New particle formation in the free troposphere: A question of chemistry and
24   timing, Science, 352, 1109-1112, 10.1126/science.aad5456, 2016.
25   Carslaw, K. S., Lee, L. A., Reddington, C. L., Pringle, K. J., Rap, A., Forster, P. M., Mann, G. W.,
26   Spracklen, D. V., Woodhouse, M. T., Regayre, L. A., and Pierce, J. R.: Large contribution of natural
27   aerosols to uncertainty in indirect forcing, Nature, 503, 67-71, 10.1038/nature12674, 2013.
28   Dal Maso, M.: Condensation and coagulation sinks and formation of nucleation mode particles in
29   coastal and boreal forest boundary layers, J. Geophys. Res., 107, 10.1029/2001jd001053, 2002.
30   Dal Maso, M., Kulmala, M., Riipinen, I., Wagner, R., Hussein, T., Aalto, P. P., and Lehtinen, K. E. J.:
31   Formation and growth of fresh atmospheric aerosols: Eight years of aerosol size distribution data
32   from SMEAR II, Hyytiälä, Finland, Boreal Environ. Res., 10, 323-336, 2005.
33   Dallósto, M., Beddows, D. C. S., Tunved, P., Krejci, R., Ström, J., Hansson, H. C., Yoon, Y. J., Park,
34   K. T., Becagli, S., Udisti, R., Onasch, T., Ódowd, C. D., Simó, R., and Harrison, R. M.: Arctic sea
35   ice melt leads to atmospheric new particle formation, Sci. Rep., 7, 10.1038/s41598-017-03328-1,
36   2017.
37   Fuchs, N. A., and Sutugin, A. G.: Highly Dispersed Aerosols, Ann Arbor Science Publ., Ann Arbor,
38   Michigan, 1970.
39   Grenfell, J. L., Harrison, R. M., Allen, A. G., Shi, J. P., Penkett, S. A., O'Dowd, C. D., Smith, M. H.,
40   Hill, M. K., Robertson, L., Hewitt, C. N., Davison, B., Lewis, A. C., Creasey, D. J., Heard, D. E.,

Hebestreit, K., Alicke, B., and James, J.: An analysis of rapid increases in condensation nuclei concentrations at a remote coastal site in western Ireland, J. Geophys. Res.: Atmos., 104, 13771-13780, 1999.

Humphries, R. S., Schofield, R., Keywood, M. D., Ward, J., Pierce, J. R., Gionfriddo, C. M., Tate, M. T., Krabbenhoft, D. P., Galbally, I. E., Molloy, S. B., Klekociuk, A. R., Johnston, P. V., Kreher, K., Thomas, A. J., Robinson, A. D., Harris, N. R. P., Johnson, R., and Wilson, S. R.: Boundary layer new particle formation over East Antarctic sea ice - Possible Hg-driven nucleation?, Atmos. Chem. Phys., 15, 13339-13364, 10.5194/acp-15-13339-2015, 2015.

Humphries, R. S., Klekociuk, A. R., Schofield, R., Keywood, M. D., Ward, J., and Wilson, S. R.: Unexpectedly high ultrafine aerosol concentrations above East Antarctic sea ice, Atmos. Chem. Phys., 16, 2185-2206, 10.5194/acp-16-2185-2016, 2016.

Jang, E., Park, K.-T., Yoon, Y. J., Kim, T.-W., Hong, S.-B., Becagli, S., Traversi, R., Kim, J., and Gim, Y.: New particle formation events observed at the King Sejong Station, Antarctic Peninsula – Part 2: Link with the oceanic biological activities, Manuscript submitted for publication, 2018.

IPCC: Climate change 2013: The physical science basis, Intergovernmental panel on Climate Change, Cambridge University Press, New York, USA, 571-740, 2013.

Ito, T.: Size distribution of Antarctic submicron aerosols, Tellus Ser. B, 45 B, 145-159, 1993.

Järvinen, E., Virkkula, A., Nieminen, T., Aalto, P. P., Asmi, E., Lanconelli, C., Busetto, M., Lupi, A., Schioppo, R., Vitale, V., Mazzola, M., Petäjä, T., Kerminen, V. M., and Kulmala, M.: Seasonal cycle and modal structure of particle number size distribution at Dome C, Antarctica, Atmos. Chem. Phys., 13, 7473-7487, 10.5194/acp-13-7473-2013, 2013.

Keil, A., and Wendisch, M.: Bursts of Aitken mode and ultrafine particles observed at the top of continental boundary layer clouds, J. Aerosol. Sci., 32, 649-660, 10.1016/s0021-8502(00)00102-6, 2001.

Kim, J., Yoon, Y. J., Gim, Y., Kang, H. J., Choi, J. H., Park, K.-T., and Lee, B. Y.: Seasonal variations in physical characteristics of aerosol particles at the King Sejong Station, Antarctic Peninsula, Atmos. Chem. Phys., 17, 12985-12999, 10.5194/acp-17-12985-2017, 2017.

Kim, J. S., Kim, Y. J., and Park, K.: Measurements of hygroscopicity and volatility of atmospheric ultrafine particles in the rural Pearl River Delta area of China, Atmos. Environ., 45, 4661-4670, 2011.

Komppula, M., Lihavainen, H., Hatakka, J., Paatero, J., Aalto, P., Kulmala, M., and Viisanen, Y.: Observations of new particle formation and size distributions at two different heights and surroundings in subarctic area in northern Finland, J. Geophys. Res. D: Atmos., 108, AAC 12-11 AAC 12-11, 2003.

Kontkanen, J., Lehtipalo, K., Ahonen, L., Kangasluoma, J., Manninen, H. E., Hakala, J., Rose, C., Sellegri, K., Xiao, S., Wang, L., Qi, X., Nie, W., Ding, A., Yu, H., Lee, S., Kerminen, V. M., Petäjä, T., and Kulmala, M.: Measurements of sub-3nm particles using a particle size magnifier in different environments: From clean mountain top to polluted megacities, Atmos. Chem. Phys., 17, 2163-2187, 10.5194/acp-17-2163-2017, 2017.

Kulmala, M., Dal Maso, M., Mäkelä, J. M., Pirjola, L., Väkevä, M., Aalto, P., Miikkulainen, P., Hämeri, K., and O'Dowd, C. D.: On the formation, growth and composition of nucleation mode particles, Tellus Ser. B, 53, 479-490, 2001.

Kulmala, M., Vehkamäki, H., Petäjä, T., Dal Maso, M., Lauri, A., Kerminen, V. M., Birmili, W., and

15

Atmospheric
Chemistry
and Physics
Discussions

McMurry, P. H.: Formation and growth rates of ultrafine atmospheric particles: A review of observations, J. Aerosol. Sci., 35, 143-176, 10.1016/j.jaerosci.2003.10.003, 2004.

Kulmala, M., Petäjä, T., Mönkkönen, P., Koponen, I. K., Dal Maso, M., Aalto, P. P., Lehtinen, K. E. J., and Kerminen, V. M.: On the growth of nucleation mode particles: source rates of condensable vapor in polluted and clean environments, Atmos. Chem. Phys., 5, 409-416, 10.5194/acp-5-409-2005, 2005.

Kyrö, E. M., Kerminen, V. M., Virkkula, A., Dal Maso, M., Parshintsev, J., Ruíz-Jimenez, J., Forsström, L., Manninen, H. E., Riekkola, M. L., Heinonen, P., and Kulmala, M.: Antarctic new particle formation from continental biogenic precursors, Atmos. Chem. Phys., 13, 3527-3546, 10.5194/acp-13-3527-2013, 2013.

Nguyen, Q. T., Glasius, M., Sørensen, L. L., Jensen, B., Skov, H., Birmili, W., Wiedensohler, A., Kristensson, A., Nøjgaard, J. K., and Massling, A.: Seasonal variation of atmospheric particle number concentrations, new particle formation and atmospheric oxidation capacity at the high Arctic site Villum Research Station, Station Nord, Atmos. Chem. Phys., 16, 11319-11336, 10.5194/acp-16-11319-2016, 2016.

O'Dowd, C. D., Hämeri, K., Mäkelä, J., Väkeva, M., Aalto, P., De Leeuw, G., Kunz, G. J., Becker, E., Hansson, H. C., Allen, A. G., Harrison, R. M., Berresheim, H., Kleefeld, C., Geever, M., Jennings, S. G., and Kulmala, M.: Coastal new particle formation: Environmental conditions and aerosol physicochemical characteristics during nucleation bursts, J. Geophys. Res.: Atmos., 107, 10.1029/2000JD000206, 2002.

Park, J., Sakurai, H., Vollmers, K., and McMurry, P. H.: Aerosol size distributions measured at the South Pole during ISCAT, Atmos. Environ., 38, 5493-5500, 10.1016/j.atmosenv.2002.12.001, 2004.

Park, K., Kim, J. S., and Seung, H. P.: Measurements of hygroscopicity and volatility of atmospheric ultrafine particles during ultrafine particle formation events at urban, industrial, and coastal sites, Environ. Sci. Technol., 43, 6710-6716, 2009.

Pierce, J. R., and Adams, P. J.: Efficiency of cloud condensation nuclei formation from ultrafine particles, Atmos. Chem. Phys., 7, 1367-1379, 10.5194/acp-7-1367-2007, 2007.

Pierce, J. R., Westervelt, D. M., Atwood, S. A., Barnes, E. A., and Leaitch, W. R.: New-particle formation, growth and climate-relevant particle production in Egbert, Canada: analysis from 1 year of size-distribution observations, Atmos. Chem. Phys., 14, 8647-8663, 10.5194/acp-14-8647-2014, 2014.

Rose, C., Sellegri, K., Velarde, F., Moreno, I., Ramonet, M., Weinhold, K., Krejci, R., Andrade, M., Wiedensohler, A., and Laj, P.: Frequent nucleation events at the high altitude station of Chacaltaya (5240m a.s.l.), Bolivia, Atmos. Environ., 102, 18-29, 10.1016/j.atmosenv.2014.11.015, 2015.

Rose, C., Sellegri, K., Moreno, I., Velarde, F., Ramonet, M., Weinhold, K., Krejci, R., Andrade, M., Wiedensohler, A., Ginot, P., and Laj, P.: CCN production by new particle formation in the free troposphere, Atmos. Chem. Phys., 17, 1529-1541, 10.5194/acp-17-1529-2017, 2017.

Shen, X., Sun, J., Zhang, X., Zhang, Y., Zhang, L., and Fan, R.: Key features of new particle formation events at background sites in China and their influence on cloud condensation nuclei, Front. Environ. Sci. Eng., 10, 05, 10.1007/s11783-016-0833-2, 2016.

Spracklen, D. V., Carslaw, K. S., Kulmala, M., Kerminen, V. M., Mann, G. W., and Sihto, S. L.: The contribution of boundary layer nucleation events to total particle concentrations on regional and global scales, Atmos. Chem. Phys., 6, 5631-5648, 10.5194/acp-6-5631-2006, 2006.

1 Stein, A. F., Draxler, R. R., Rolph, G. D., Stunder, B. J. B., Cohen, M. D., and Ngan, F.: Noaa's hysplit
2   atmospheric transport and dispersion modeling system, Bull. Amer. Meteorol. Soc., 96, 2059-2077,
3   10.1175/bams-d-14-00110.1, 2015.
4 Twomey, S.: The Influence of Pollution on the Shortwave Albedo of Clouds, J. Atmos. Sci., 34, 1149-
5   1152, 10.1175/1520-0469(1977)034<1149:Tiopot>2.0.Co;2, 1977.
6 Virkkula, A., Asmi, E., Teinilä, K., Frey, A., Aurela, M., Timonen, H., Mäkelä, T., Samuli, A., Hillamo,
7   R., Aalto, P. P., Kirkwood, S., and Kulmala, M.: Review of aerosol research at the Finnish Antarctic
8   research station Aboa and its surroundings in Queen Maud Land, Antarctica, Geophysica, 45, 163-
9   181, 2009.
10 Warren, D. R., and Seinfeld, J. H.: Prediction of aerosol concentrations resulting from a burst of
11   nucleation, J Colloid Interf. Sci., 105, 136-142, https://doi.org/10.1016/0021-9797(85)90356-X,
12   1985.
13 Weingartner, E., Nyeki, S., and Baltensperger, U.: Seasonal and diurnal variation of aerosol size
14   distributions (10 < D < 750 nm) at a high-alpine site (Jungfraujoch 3580 m asl), J. Geophys. Res.:
15   Atmos., 104, 26809-26820, 1999.
16 Weller, R., Schmidt, K., Teinilä, K., and Hillamo, R.: Natural new particle formation at the coastal
17   Antarctic site Neumayer, Atmos. Chem. Phys., 15, 11399-11410, 10.5194/acp-15-11399-2015,
18   2015.
19 Willis, M. D., Burkart, J., Thomas, J. L., Köllner, F., Schneider, J., Bozem, H., Hoor, P. M., Aliabadi,
20   A. A., Schulz, H., Herber, A. B., Leaitch, W. R., and Abbatt, J. P. D.: Growth of nucleation mode
21   particles in the summertime Arctic: A case study, Atmos. Chem. Phys., 16, 7663-7679,
22   10.5194/acp-16-7663-2016, 2016.
23 Woo, K. S., Chen, D. R., Pui, D. Y. H., and McMurry, P. H.: Measurement of Atlanta aerosol size
24   distributions: Observations of ultrafine particle events, Aerosol Sci. Technol., 34, 75-87, 2001.
25 Yli-Juuti, T., Riipinen, I., Aalto, P. P., Nieminen, T., Maenhaut, W., Janssens, I. A., Claeys, M., Salma,
26   I., Ocskay, R., Hoffer, A., Imre, K., and Kulmala, M.: Characteristics of new particle formation
27   events and cluster ions at K-puszta, Hungary, Boreal Environ. Res., 14, 683-698, 2009.
28 Yoon, Y. J., O'Dowd, C. D., Jennings, S. G., and Lee, S. H.: Statistical characteristics and predictability
29   of particle formation events at Mace Head, J. Geophys. Res.: Atmos., 111, 10.1029/2005JD006284,
30   2006.
31 Yu, F., and Luo, G.: Oceanic dimethyl sulfide emission and new particle formation around the coast of
32   antarctica: A modeling study of seasonal variations and comparison with measurements,
33   Atmosphere, 1, 34-50, 10.3390/atmos1010034, 2010.
34
35

Atmospheric
Chemistry
and Physics
Discussions

1
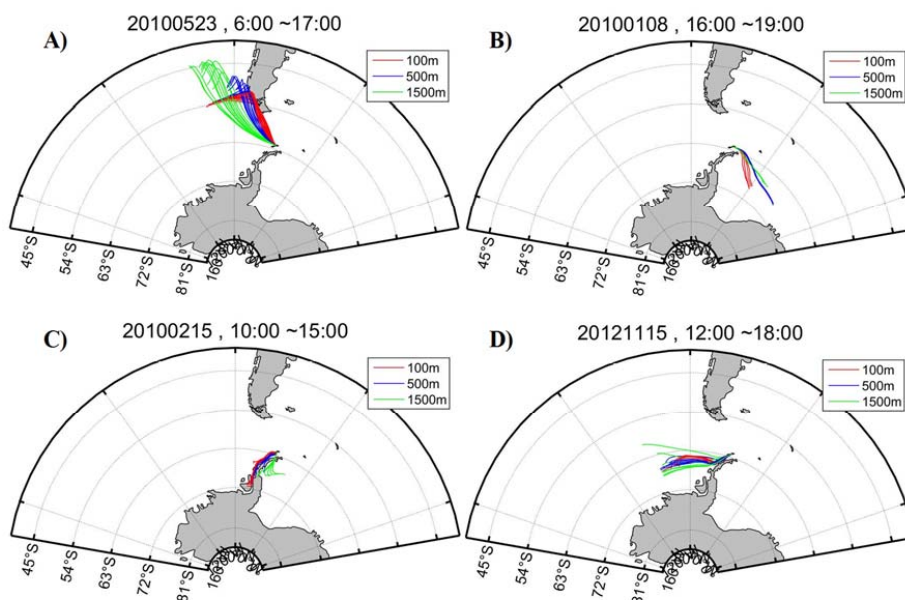
Figure 1. Example of the four cases considering to the air mass origin and pathway: (a) South America, (b) Weddell Sea, (c) Antarctic Peninsula, and (d) Bellingshausen Sea. Typical 48-h air mass backward trajectories were analyzed, ending at heights of 100m (Red line), 500m (Blue line) and 1500m (Green line) above the ground level of the sampling site.
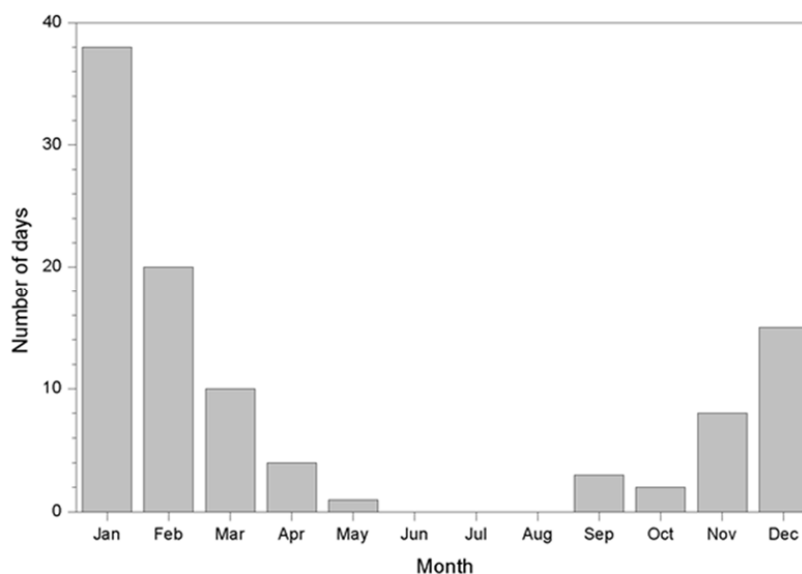
1

2

3

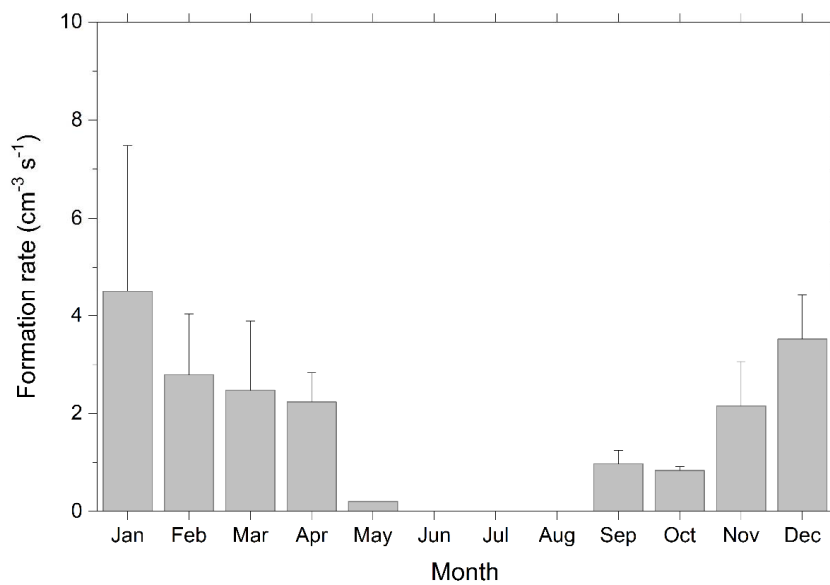Figure 2. Monthly variation in the number of NPF days between March 2009 and December 2016.

5

6

Atmospheric
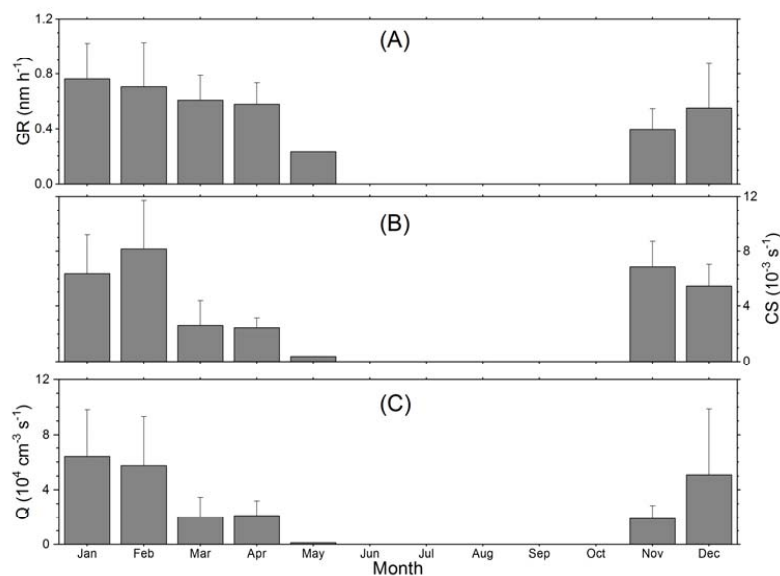Chemistry
and Physics
Discussions

Open Access

1

2

3

4   Figure 3. Monthly variation in the formation rate. The error bars represent standard deviation

5

6

Atmospheric
Chemistry
and Physics
Discussions

1

2

3

4 Figure 4. Monthly variation in (a) the growth rates (GR) of nucleation mode particles ranging from 10

5 nm to 25 nm, (b) the condensation sink (CS), and (c) the source rate of condensable vapor (Q). The

6 error bars represent standard deviation.

7

8

Atmospheric
Chemistry
and Physics
Discussions

1
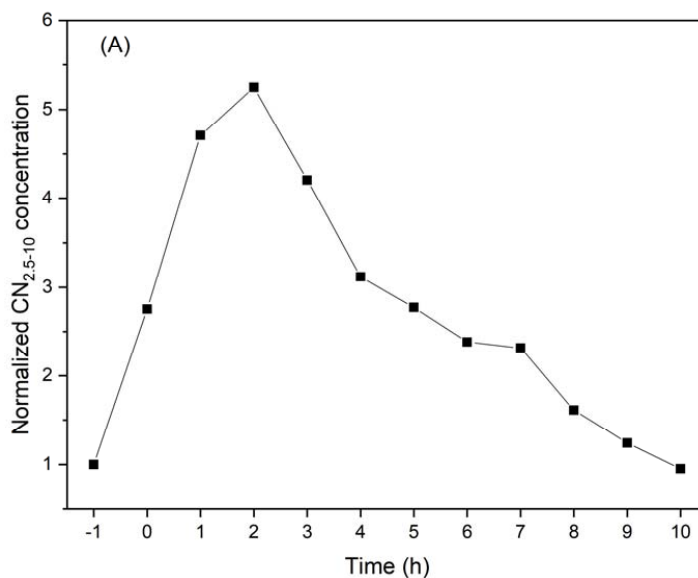
2
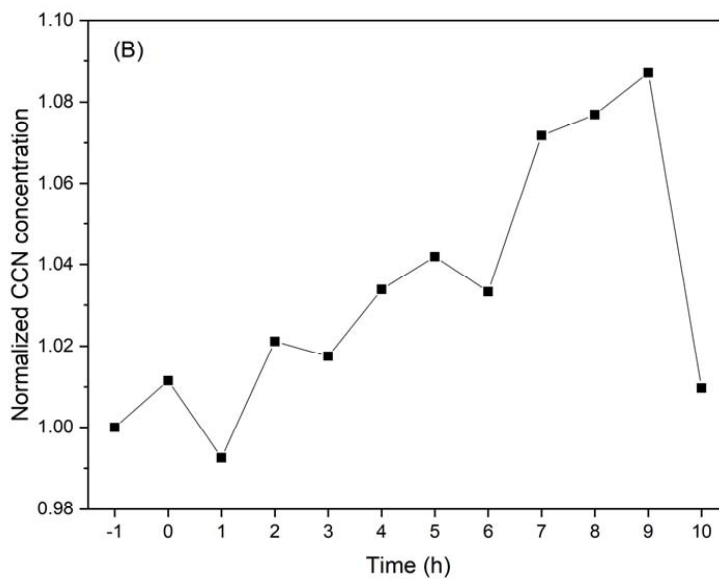
3

4   Figure 5. Variation in normalized (a) CN$_{2.5-10}$ and (b) CCN concentration with time. The zero in the x-

5   axis indicates the start time of the NPF events.

Atmospheric
Chemistry
and Physics
Discussions

Open Access

1

2

3
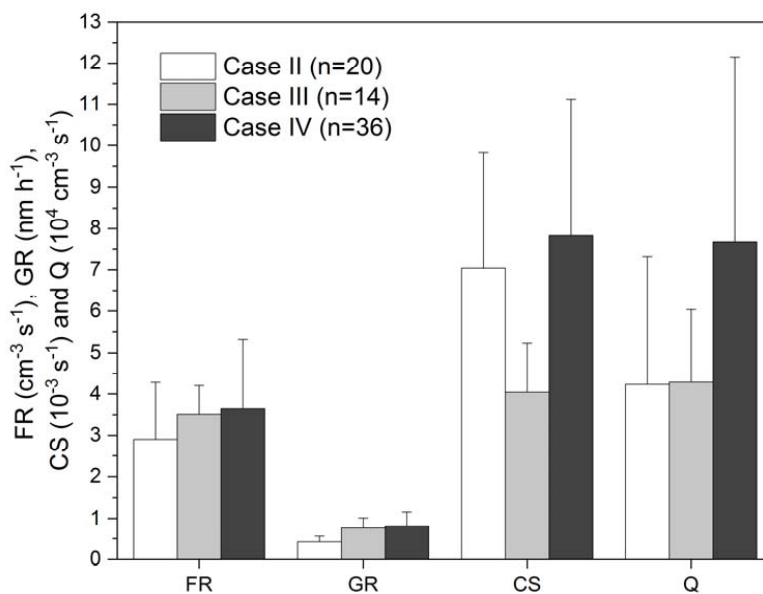
Figure 6. Comparison of NPF characteristics including the formation rate (FR), growth rate (GR),
condensation sink (CS) and source rate of condensable vapors (Q) depending on the origins and
pathway of air masses during the astral summer period. The error bars represent standard deviation.

7

8

1

2

3
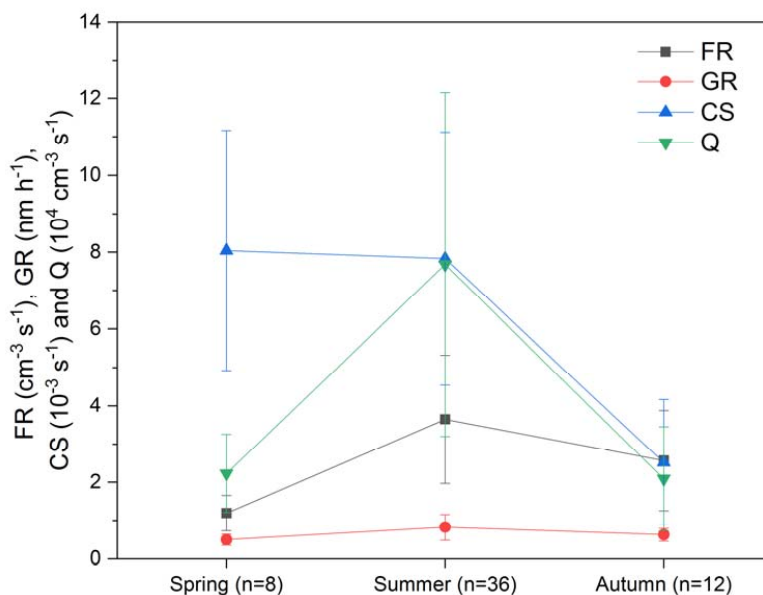
Figure 7. Seasonal characteristics of parameters related to NPF events in which the air masses originated from the Bellingshausen Sea. FR, GR, CS, and Q refer to formation rate, growth rate, condensation sink, and source rate of condensing vapor, respectively. The error bars represent standard deviation.

8

9

1

2   Table 1. Summary of data acquisition rate for each instrument during the analysis periods

Measurement parameter	Instrument	Data acquisition rate(%)
Number concentration of particle larger than 2.5 nm	CPC (TSI 3776)	80.7
Number concentration of particle larger than 10 nm	CPC (TSI 3772)	79.5
Size distribution	SMPS	40.3
CCN concentrations	CCNC	36.4

3
4
5

6   Table 2. Event statistics classified by using total concentration data obtained from two CPCs

	Days	Percentage of total days
NPF events	101	6.1
Non events	1554	93.9
Total	1655	

7

Atmospheric
Chemistry
and Physics
Discussions

1 Table 3. Summary of the formation rates observed at different sampling site in Antarctica and in other continents. DMPS, SMPS, and CPC mean
2 differential mobility particle sizer, scanning mobility particle sizer, and condensation particle counter, respectively.
3

Site	Period	Method	Formation rates (cm^{-3} s^{-1})		References
King Sejong (Antarctic Peninsula)	03/2009 ~ 12/2016	Two CPCs (TSI 3772 & TSI 3776)	$J_{2.5-10}$	2.79	This study
Syowa (Antarctica)	08/1978 ~ 12/1978		J_{10}	3.8×10^{-4}	Ito, 1993
Dome C (Antarctica)	12/2007 ~ 11/2009	DMPS	J_{10}	0.038	Järvinen et al., 2013
Aboa (Antarctica)	01/2010	DMPS	J_{10}	0.003 ~ 0.3	Kyrö et al., 2013
Neumayer (Antarctica)	20/01/2012 ~ 26/03/2012 01/02/2014 ~ 30/04/2014	SMPS	J_{3-25}	0.02 ~ 0.1	Weller et al., 2015
Värriö (Sub Arctic)	12/1997 ~ 07/2001	DMPS	J_{10}	0.38	Dal Maso, 2002
Hyytiälä (Rural)	1996 ~ 2003	DMPS	J_{3-25}	0.61	Dal Maso et al., 2005
Mace Head (Coastal)	1996 ~ 1997	Two CPCs (TSI 3022 & TSI 3025)	J_{3-10}	$10^2 \sim 10^4$	Grenfell et al., 1999
Jungfraujoch (Remote)	03/1997 ~ 05/1998	SMPS	J_{10}	0.14	Weingartner et al., 1999
Dresden area (Rural)	1996 ~ 1998	Two CPCs (UCPC & CPC)	J_{10}	110	Keil and Wendisch, 2001
Atlanta (Urban)	08/1998 ~ 08/1999	Nano-SMPS	J_3	10 ~ 15	Woo et al., 2001
Shangdianzi (Rural)	03/2008 ~ 12/2013	DMPS	J_3	6.3	Shen et al., 2016

Atmospheric
Chemistry
and Physics
Discussions
Open Access

1   Table 4. NPF event classification statistics using size distribution results. Type A refers to days in which

2   the formation and growth of particles were clear. Type B refer to days in which the formation occurred

3   but the growth was not clear. Type C refers to days in which the event occurrence was unclear.

	Days	Percentage of NPF days
Type A	2	2.0
Type B	37	36.6
Type C	62	61.4
Total	101	

4

5   Table 5. Summary of NPF characteristic statics depending on the air mass origin. FR is the formation

6   rate, GR is the growth rate, CS is the condensation sink, and Q is the source rate of condensable vapor.

7   Case I, Case II, Case III, and Case IV refer to the origin and pathway of air masses from South America,

8   the Weddell Sea, the Antarctic Peninsula, and the Bellingshausen Sea, respectively.

	NPF days	FR (cm^{-3} s^{-1})	GR (nm h^{-1})	CS (10^{-3} s^{-1})	Q (10^4 cm^{-3} s^{-1})
Case I	3				
Case II	24	2.81 ± 1.29	0.41 ± 0.15	6.95 ± 2.65	3.87 ± 2.90
Case III	16	3.10 ± 0.80	0.77 ± 0.25	4.19 ± 1.30	4.29 ± 1.75
Case IV	56	3.08 ± 1.55	0.76 ± 0.30	6.79 ± 3.20	6.20 ± 4.08
Undefined	2				

9